# Hydrophilic Selective Nanochannels Created by Metal Organic Frameworks in Nanofiltration Membranes Enhance Rejection of Hydrophobic Endocrine Disrupting Compounds

Ruobin Dai,[†] Hao Guo,[‡] Chuyang Y. Tang, [‡,§,£] Mei Chen,[†] Jiayi Li,[†] Zhiwei Wang[†,*]

[†] State Key Laboratory of Pollution Control and Resource Reuse, Shanghai Institute of Pollution Control and Ecological Security, School of Environmental Science and Engineering, Tongji University, Shanghai 200092, China

[‡] Department of Civil Engineering, the University of Hong Kong, Pokfulam Road, Hong Kong S.A.R., China

[§] UNESCO Centre for Membrane Science and Technology, School of Chemical Engineering, University of New South Wales, Sydney, New South Wales 2052, Australia

[£] UNSW Water Research Centre, School of Civil and Environmental Engineering, University of New South Wales, Sydney, New South Wales 2052, Australia

[*] To whom all correspondence should be addressed.

Tel.: +86-21-65975669, Fax: +86-21-65980400, E-mail address: zwwang@tongji.edu.cn

Revised Manuscript Submitted to *Environmental Science & Technology* (clean version)

## ABSTRACT

Rejection of endocrine-disrupting compounds (EDCs) by thin film composite (TFC) polyamide membranes remains to be a challenging issue in wastewater reclamation applications due to the unfavourable hydrophobic interaction between EDCs and membrane. Herein, we investigated the incorporation of hydrophilic metal organic frameworks (MOFs) into polyamide layer to create water/EDCs selective nanochannels for enhancing EDCs rejection. Using MIL-101(Cr) MOF as a nanofiller, the water flux of MOF0.20 TFC membrane (0.20 wt/v % MOF in *n*-hexane) was 2.3 times of that of the control. The rejection rates against EDCs involving methylparaben, propylparaben, benzylparaben and bisphenol A (BPA) by MOF0.20 were also significantly higher than the respective values of the control membrane, with the water/EDC selectivity (e.g., $A/B_{BPA}$) of MOF0.20 approximately doubled compared to that of the control. Further single salt rejection and gold nanoparticle filtration tests confirmed that the hydrophilic nanochannels created by MOFs played a critical role in membrane transport, accounting for the significant enhancement of EDCs rejection of the modified TFC membrane. This study demonstrates a promising membrane modification protocol using hydrophilic MOFs for achieving selective removal of EDCs and high-efficient wastewater reclamation using TFC membranes.

## TOC art

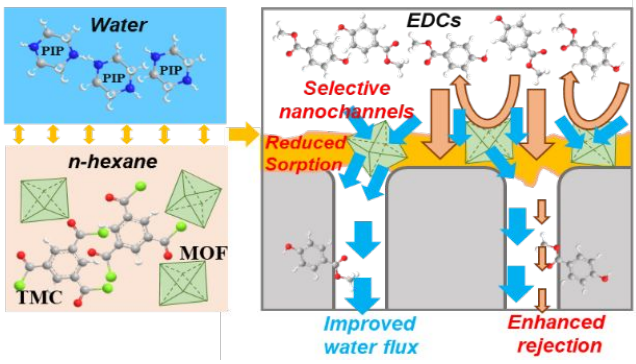
Water
PIP
PIP
PIP
n-hexane
MOF
TMC
EDCs
Selective
nanochannels
Reduced
Sorption
Improved
water flux
Enhanced
rejection

## INTRODUCTION

Wastewater reclamation, using membrane-based processes such as reverse osmosis (RO) and nanofiltration (NF), is of great importance to address the grand challenge of water scarcity[1–4]. Although thin film composite polyamide NF and RO membranes are capable of removing the majority of pollutants in wastewater (including inorganic salts)[5–7], they often show unfavourable rejection towards neutral and hydrophobic organic micropollutants such as endocrine disrupting compounds (EDCs)[8–11], which are of ubiquitous occurrence in contaminated waters[12–14]. Due to the hydrophobic interaction between EDCs and membrane[9,10,15], the rejection rate of some EDCs by existing polyamide NF/RO membranes can be even lower than 20%[16–19]. As EDCs have been reported to adversely affect endocrine and developmental system of mammals even at trace concentrations[20,21], their presence in the NF/RO permeate might have a significant health risk in wastewater reclamation.

Hydrophilic modification of membrane surface has been shown effective to enhance the rejection of EDCs, as a result of the reduced sorption and transmission of EDCs through the membrane[9,10]. It has been reported that coating polydopamine on a commercial NF membrane[10] led to improved membrane rejection of EDCs. Similarly, surface coating by tannic acid (TA)-iron (Fe) complex[22], a faster and greener coating method, has been also found to enhance rejection of EDCs. However, one important concern for the coating approach is the loss of water permeability of membrane [10,22,23], e.g., up to 40% for the case of 4 h polydopamine coating on NF90[10], which in turn results in a significant increase of energy consumption in water reuse applications[24]. Therefore, it is of great importance to explore membrane modification techniques for improving EDCs rejection without compromising water permeability.

Incorporating nanoparticles (NPs) into the polyamide rejection layer, i.e., thin-film nanocomposite (TFN) membrane[25], offers a potential solution for improving water/EDCs selectivity. It has been reported that the incorporation of NPs and metal organic frameworks (MOFs) into polyamide membrane has the potential to overcome the permeability-selectivity trade-off[26–28] by simultaneously enhancing the membrane permeability and salt rejection rate[27,29]. Compared to inorganic NPs, the highly porous structure, adjustable pore size, and good compatibility to polyamide make MOFs an emerging alternative for advancing membrane performance[29–34]. However, existing literature on MOF-based TFN membranes focuses primarily on water permeability and salt rejection. In contrast, the removal of trace organic contaminants such as EDCs, a critical aspect in water reuse[33], has not been explored for MOF-TFN membranes.

In this study, we hypothesize that incorporation of hydrophilic MOFs into polyamide layer can simultaneously improve water permeability and EDCs selectivity, thanks to the creation of highly selective nanochannels in the resulting TFN membranes. Moreover, the possible formation of hydrophilic membrane surface can also reduce the sorption and passage of EDCs across the membrane. A mesoporous MOF, Cr-BDC MOFs MIL-101(Cr) (Figure S1) with 1.2 nm pentagonal/1.6 nm hexagonal openings, was selected due to its hydrophilic and water stable nature. Its large pore volumes and surface area provide abundant water channels[35]. In this work, MOF MIL-101(Cr) was incorporated into polyamide NF membrane under various loadings, and its effects on membrane separation performance including water transportation and rejection of EDCs were studied. The roles of nanochannels created by the MOFs in membrane separation were systematically investigated. The results demonstrate a promising membrane

modification strategy for achieving selective removal of EDCs and thus high-efficient wastewater reclamation.

## MATERIALS AND METHODS

**Materials and Chemicals.** Commercially available polyethersulfone (PES) ultrafiltration membranes (LX-300K, Synder Filtration) with a molecular weight cutoff of 300 kDa were used as the substrate. The PES membranes were pre-treated by 20% isopropanol for 30 min and then immersed in deionized (DI) water for 24 h prior to use. The MOF MIL-101(Cr) was synthesized according to Férey et al[34]. Before characterization and further use, MIL-101(Cr) was vacuum activated overnight at 120°C. Piperazine (PIP, 99%), trimesoyl chloride (TMC, 98%), triethylamine (TEA, 99%), sodium hydroxide (NaOH, ≥98%), and *n*-hexane (≥98%) from Macklin® were used for interfacial polymerization (IP) to form the polyamide selective layer. Four EDCs, including methylparaben (≥99%), propylparaben (99%), benzylparaben (≥99%), and bisphenol A (BPA, ≥99%), were obtained from Macklin®. The physicochemical properties of the EDCs are summarized in Table S1. Neutral organic molecules (erythritol, xylose, and dextrose) from Aladdin® were used as surrogates for determining the effect of size exclusion. Citrate-stabilized 5 nm gold nanoparticles (GNPs) solution was purchased from BBI solutions (UK).

**Membrane Fabrication.** TFC NF membranes were fabricated by forming a PA selective layer on top of the PES support membrane via IP. Specifically, the PES membrane for reaction was cut into pieces (10 cm ×15 cm) and fixed between two identical custom-designed stainless-steel frames, with the top layer facing upward. An aqueous solution of 1.0 wt% PIP with 0.5 wt%

TEA and 0.15 wt% NaOH as additives was poured onto the surface of PES membrane with a contact time of 2 min. The excess solution was gently removed from the membrane surface using filter papers. The top surface of the membrane was then exposed to a 0.15 wt% TMC/*n*-hexane solution for 30 s and the solution was subsequently poured off, followed by vertically draining the membrane for another 2 min. The composite membrane was then thoroughly rinsed by *n*-hexane and DI water, and stored in DI water at 4°C. The TFC membrane fabricated was denoted as NFcontrol.

For MIL-101(Cr)/polyamide thin film nanocomposite (TFN) membranes, 0.10 to 0.25 wt/v % MIL-101(Cr) was dispersed in the TMC/*n*-hexane solution via ultrasonication at room temperature for 30 min prior to IP. The other reaction procedures were the same as those for making TFC membranes. The MOF incorporated TFN membranes are denoted as MOF0.10, MOF0.15, MOF0.20, MOF0.25, respectively, corresponding to the MIL-101(Cr) loading mass.

**Membrane Characterization.** Membrane surface morphology was observed by a field emission scanning electron microscopy (FESEM, Hitachi S-4800) at 5.0 kV. Transmission electron microscopy (TEM, FEI 120kV) was used to examine membrane cross-section structure. Briefly, dry membrane samples were embedded in epoxy resin. After curing at 70°C overnight, the resin block was cross-sectioned by an ultramicrotome (Leica UC7) into TEM sections of 70-90 nm in thickness. These sections were immobilized onto a copper grid and further examined by TEM. Atomic force microscopy (AFM), X-ray photoelectron spectroscopy (XPS), attenuated total reflectance Fourier transform infrared spectroscopy (ATR-FTIR) and contact angle measurements for surface of the membranes were detailed in our previous work[26]. Two probing liquids including water and diiodomethane were used to obtain surface energy of the

membrane. Zeta potential of membrane surface was evaluated by an electrokinetic analyzer for solid surface analysis (SurPASS$^{TM}$ 3, Anton Paar) from pH 3 to 10 in an automatic pH scan mode.

**Cross-flow Filtration Tests.** A laboratory-scale cross-flow membrane filtration setup (Figure S2) was used to perform the rejection of single salt, neutral solutes, and EDCs. The effective filtration area of the cross-flow cell was 20.02 $cm^2$. A 10 L DI water was recirculated for 4 h for membrane precompaction at 10 bar with a cross-flow velocity of 20.0 cm/s, until the permeate flux was stable. The feed solution temperature was kept constant at 25.0 ± 0.5°C. Pure water flux was then measured at 8 bar.

Single salt rejections were evaluated using 10 mM of NaCl, $CaCl_2$ and $Na_2SO_4$ solutions at 8 bar after precompaction, respectively. Feed solution pH was adjusted to 7.0 ± 0.1 before rejection experiments. The permeate and feed samples were obtained after the system reached equilibrium for 1 h at each condition, and analyzed using a conductivity meter (DDSJ-308F, INESA instrument). The membrane rejection was calculated by comparing the ion concentration in the feed ($C_f$) and permeate ($C_p$) samples ($R$=1-$C_p/C_f$).

EDCs rejections were tested under a concentration of 200 μg/L for each compound at 8 bar via introducing 1 g/L stock solutions of EDCs. The experiments were performed for 10 h to ensure the sorption of EDCs by membranes to reach equilibrium[10]. The permeate and feed samples were then collected for EDC quantification.

**Sorption Tests.** The EDC-filtered membranes were cut into coupons of 2 cm × 3 cm and gently rinsed with DI water. The membrane coupons were then put into 50 mL 50% methanol solution for extraction of EDCs at 120 rpm for 24 h. The extracted samples were then collected for EDC

analysis.

**Analytical Method for EDCs.** The concentrations of EDCs were determined using a high-performance liquid chromatography tandem quadrupole mass spectrometry (LC-MS/MS, Thermo TSQ Quantum). The detailed procedures are documented in supporting information (SI), Section S2.

**Gold Nanoparticles (GNPs) Filtration Tests.** Dynamic GNPs filtration tests were performed in the dead-end filtration Amicon® cell (type 8050, effective area 13.4 $cm^2$) without stirring. The membrane was pre-compacted using DI water at 5.0 bar for 30 min. Then 40 mL of a dilute solution of GNPs in DI water ($1.0 \times 10^{12}$ particles/mL) was carefully added into the cell for filtration experiments at 5.0 bar. Static tests (without pressure) were performed in the cell with the same diluted GNPs solution for 12 h exposure. All tested membranes were dried at 40°C for 6 h before preparing samples for cross-sectional TEM characterization.

## RESULTS AND DISCUSSION

**Membrane characterization.** The synthesized nanofillers MIL-101(Cr), with porous nature (BET surface area = 2511.7 $m^2/g$), have nanometric crystal size and narrow particle size distribution around 200 nm (Figure S3), in agreement with previous studies[32,34,35]. TEM cross-sectional images (Figure 1a-d) and SEM images (Figures S4 and S5) of the NFcontrol and various MOF-TFN membranes confirmed the successful loading of MOF nanoparticles into polyamide. The amounts of the MOF nanoparticles on membrane surface increased with the increase of MIL-101(Cr) dosages in TMC/*n*-hexane (Figures S4 and S5). The results of XPS survey revealed the presence of chromium on MOF-TFN membranes (Figure 1e and Table S2).

For MOF0.20, a Cr content of 1.2% was detected, which corresponds to 9.0 wt% MIL-101(Cr) particles in the top polyamide layer based on the formula of MIL-101(Cr) $[Cr_3O(OH)(H_2O)_2[C_6H_4(CO_2)_2]_3 \cdot 25H_2O]$[32]. The maximum Cr content of 3.4% was observed for MOF0.25, much greater than that of MOF0.20, potentially due to the particle aggregation for MOF0.25 at the highest MOF loading. The high-resolution XPS spectra (Figure 1g, h) for O 1s provided further evidence of the presence of MIL-101(Cr) on the membrane surface: (1) an additional peak at 534.3 eV associated with chromium species containing coordination bond (C-O*-Cr) was observed for MOF0.20; (2) the ratio of N-C=O* to O*-C=O for MOF0.20 decreased compared to that of NFcontrol, possibly associated with the carboxylic acid groups of MIL-101(Cr) and/or the decrease of crosslinking degree. The enhanced peak intensity of peak at 1404 $cm^{-1}$ after MOF incorporation in ATR-FTIR characterization (Figure 1f) also validated the increase of C−O bond of carboxylic groups.

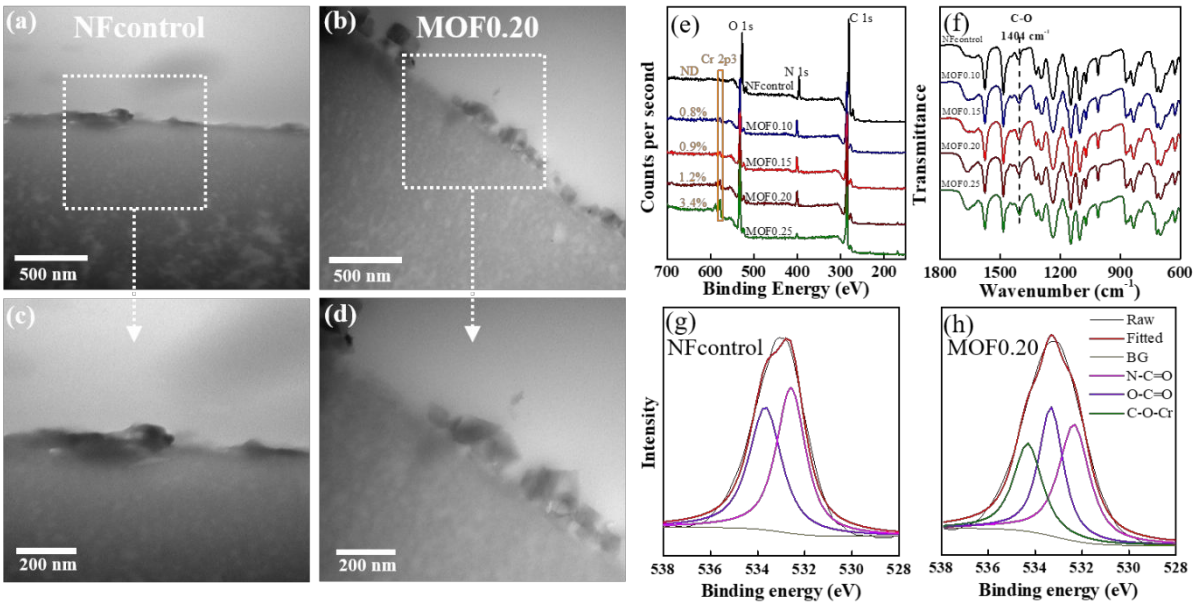


**Figure 1.** Characterization of fabricated membranes: (a-d) TEM cross-sections of the NFcontrol and MOF0.20 membranes; (e) XPS spectra of top surface of membranes; (f) ATR-FTIR spectra of the top surface of membranes; (g, h) XPS analysis of oxygen 1s in a high-resolution for NFcontrol and MOF0.20 membranes.

Loading MIL-101(Cr) decreased the water contact angle of the membrane from 52.3 ± 0.8° (NFcontrol) to 31.8 ± 4.8° for MOF0.25 (Table 1). Surface energy analysis indicates that the incorporation of MOF increased the total surface energy, which was mainly ascribed to the increase in the polar components. These results indicated that the surface of membranes became more hydrophilic after MOF incorporation.

**Table 1.** Membrane surface properties of NFcontrol and MOF-TFN membranes

| Membrane | Water contact angle (°) | Diiodomethane contact angle (°) | Surface energy (mN/m) | | | Roughness $R_a$ (nm) |
|---|---|---|---|---|---|---|
| | | | Total | Polar | Dispersive | |
| NFcontrol | 52.3 ± 0.8 | 25.5 ± 0.7 | 58.2 ± 0.6 | 12.2 ± 0.3 | 45.7 ± 0.3 | 26.7 ± 9.7 |
| MOF0.10 | 46.7 ± 0.6 | 19.0 ± 1.0 | 62.4 ± 0.2 | 14.3 ± 0.5 | 48.1 ± 0.3 | 36.2 ± 10.3 |
| MOF0.15 | 41.2 ± 3.2 | 18.6 ± 0.6 | 64.7 ± 1.1 | 16.5 ± 1.2 | 48.2 ± 0.2 | 46.7 ± 12.8 |
| MOF0.20 | 35.3 ± 0.1 | 18.2 ± 0.3 | 68.2 ± 0.1 | 19.9 ± 0.1 | 48.3 ± 0.1 | 47.3 ± 20.6 |
| MOF0.25 | 31.8 ± 4.8 | 15.3 ± 2.0 | 70.3 ± 2.3 | 21.2 ± 1.8 | 49.0 ± 0.4 | 52.3 ± 24.0 |

Note: Contact angle values have been corrected for the roughness effect using the Wenzel equation[36]. The results were calculated based on at least three measurements.

**MOF dominates membrane transport properties.** Figure 2(a, b) shows that increasing the MIL-101(Cr) loading significantly enhanced membrane water permeability together with mild reduction in NaCl rejection (with the exception of the MOF0.25 membrane). Specifically, the MOF0.20 membrane showed a high water permeability of 39.5 ± 3.2 L $m^{-2}$ $h^{-1}$ $bar^{-1}$, which was approximately 2.3 times compared to that of the control TFC membrane (Figure 3a). The size of nanochannels inside the MOFs were 1.2/1.6 nm, while in comparison, the average pore size

of polyamide active layer was estimated to be ~0.60 nm based on the rejection tests of multiple neutral solutes (SI, Section S8). Therefore, the water molecules may tend to pass preferentially through the nanochannels of MIL-101(Cr) of larger size (1.2/1.6 nm).

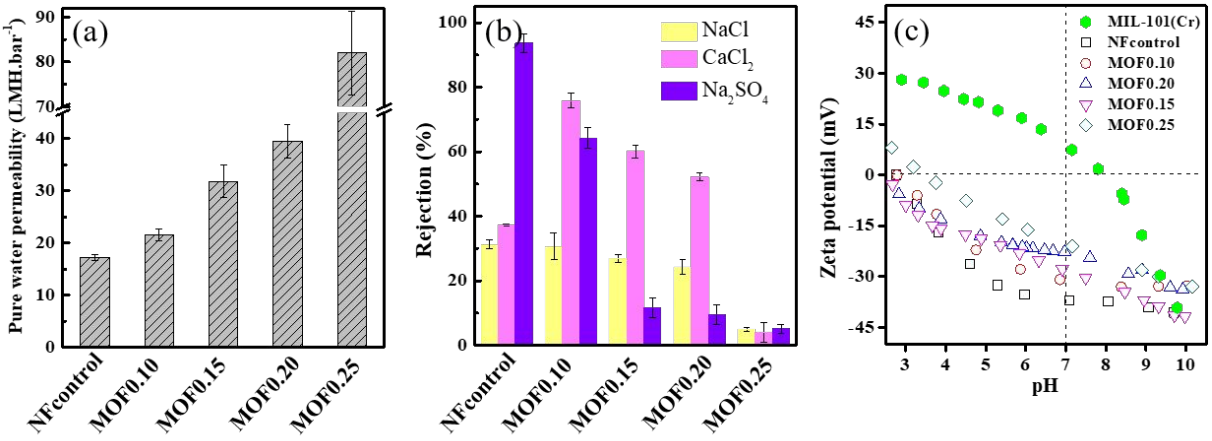


**Figure 2.** Evidence for dominance of MOFs on membrane rejection performance: (a) Pure water flux; (b) single salt (NaCl, $CaCl_2$ and $Na_2SO_4$) rejections of NFcontrol and MOF-TFN membranes; (c) Zeta potential as a function of pH of MIL-101(Cr) suspension, NFcontrol and MOF-TFN membranes. The error bars represent the standard deviations of the results of at least three independent tests.

Rejection of asymmetric charged salts, such as $CaCl_2$ and $Na_2SO_4$, is governed by the ions with higher valency (i.e., $Ca^{2+}$ for $CaCl_2$ and $SO_4^{2-}$ for $Na_2SO_4$), because the rate of salt transport is controlled by the electrostatic repulsive or attractive interactions between the ion and the membrane[37,38]. Therefore, we used $CaCl_2$ and $Na_2SO_4$ to probe the role of MIL-101(Cr) in membrane separation properties. Interestingly, compared to NFcontrol, the MOF incorporated membranes MOF0.10, MOF0.15 and MOF0.20 had decreased $Na_2SO_4$ but increased $CaCl_2$ rejections, which is consistent with the positively charged nature of MIL-101(Cr) (Figure 2c). However, the surface charge of all membranes was still negative at neutral pH. This shift in rejection behavior, along with the dramatic increase in water permeability, reveals the important role of MOFs in MOF-TFN membranes, *i.e.*, nanochannels (pores) in MOFs may dominate the

membrane transport properties. A recent study[39] also suggests the possibility of additional selective nanochannel formation around hydrophilic nanofillers. The rejections of $CaCl_2$ and NaCl decreased slightly with the increase of MOF concentrations from 0.10 to 0.20 wt/v %, which might also be partially attributed to the increased membrane pore size and thus reduced size exclusion effect (as evidenced by the decreased rejection of the neutral hydrophilic probe molecule dextrose as shown in Figure S7).

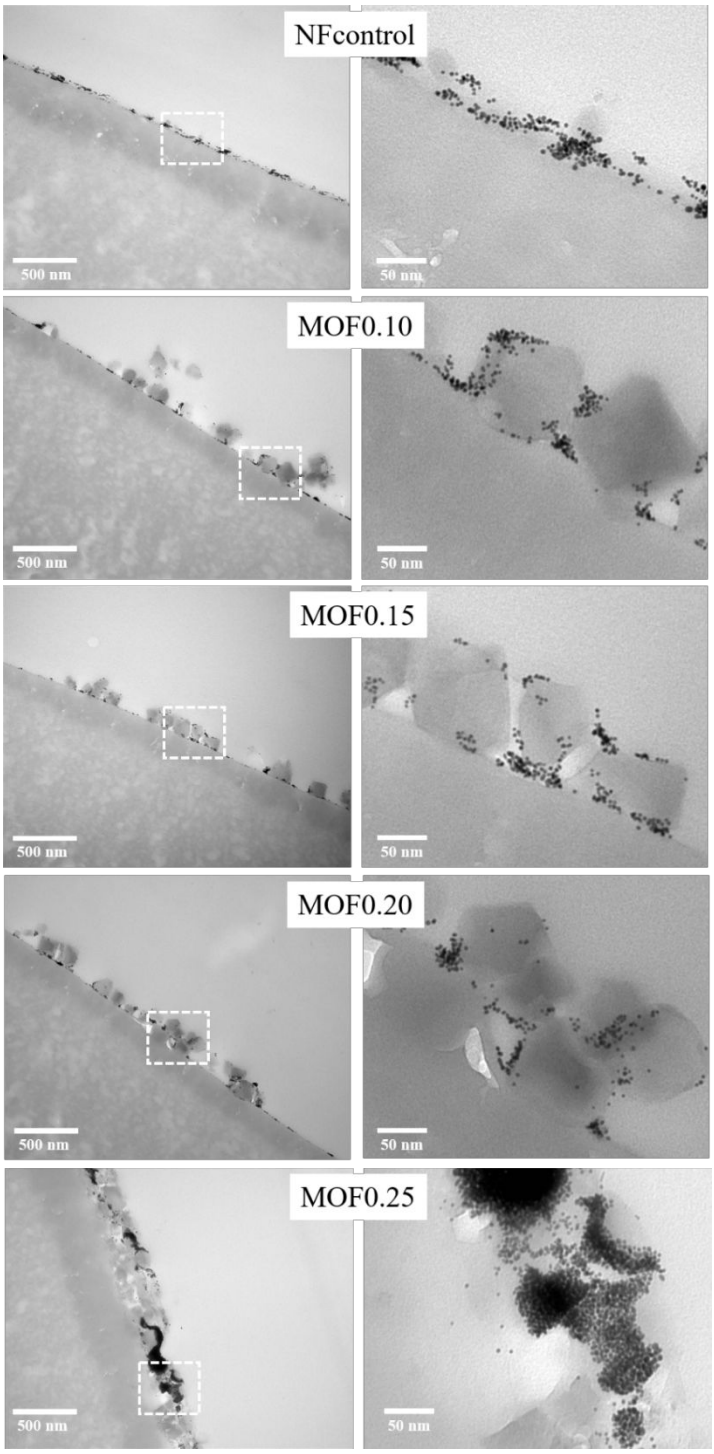


**Figure 3.** Cross-section TEM images showing gold nanoparticle deposition on the surfaces of NFcontrol and MOF-TFN membranes after 10-min filtration tests ($1.0 \times 10^{12}$ particles/mL, 25°C, 5 bar)

To further verify the hypothesis that the nanochannels (pores) of MOFs dominate the membrane transport properties, we used gold nanoparticles (GNPs) in combination with TEM

to visualize the spatial distribution of sites for water permeation in the MOF-TFN membranes (Figure 3). Due to the fine size of GNPs, they are expected to closely follow the streamlines and are therefore useful markers for water transport pathways [40,41]. Cross-section TEM micrographs of GNP-filtrated membranes revealed that the deposition of GNPs was less uniformly distributed for the MOF-TFN membrane surfaces compared with NFcontrol membrane. There was a clear tendency for GNPs to cluster around the MOF particles. In contrast, under static test conditions (without water flow through the membrane), GNPs deposition was rarely observed (Figure S8). These results provide strong evidence supporting the existence of relatively higher water permeability sites (nanochannels) of the MIL-101(Cr) MOFs. Therefore, the significant enhancement in water permeability (Figure 3a) should be attributed to the nanochannels inside the MOFs, acting as shortcuts for water transport with significantly reduced membrane hydraulic resistance.

For MOF0.25, large quantities of GNPs were enriched around MOFs and some GNPs even penetrated into the substrate, which did not happen for other membranes. It indicates the presence of defects on the surface of MOF0.25, which agrees well with the severe loss of ion rejections for this membrane (Figure 2b). The defects can be caused by the aggregation of MOFs[26,28,32], as MIL-101(Cr) cannot be dispersed completely in TMC/n-hexane when the MOF concentration reached 0.25 wt/v %.

**Rejection of EDCs.** Figure 4a presents the rejection of EDCs by NFcontrol and MOF-TFN membranes. Except for defect-laden MOF0.25, the MOF incorporation significantly improved membrane rejection for all tested EDCs, and the highest rejection was achieved by MOF0.20.

The rejection rates against methylparaben, propylparaben, benzylparaben and BPA by MOF0.20 were 47.4%, 45.9%, 51.1% and 79.8%, respectively. These values were significantly higher than those of NFcontrol (27.7%, 25.2%, 31.3% and 64.9%, respectively). The MOF0.20 presented nearly 2 times larger water/EDC selectivity (e.g., $A/B_{BPA}$) compared to NFcontrol membrane (Figure 4b), despite that the permeability of EDCs for MOF0.20 remained comparable to that of NFcontrol (Figure S9). In contrast, largely ascribed to the defects, MOF0.25 membrane showed unfavorable EDCs rejection (~10%), as well as the lowest water/EDC selectivity. Notably, for most membranes (NFcontrol, MOF0.10-0.20), the rejection rate of EDCs showed opposite tendency compared to that of molecular probe (dextrose, 180 Da), whose rejection decreased with the increase of MOF loadings (Figure S7). Since the rejection of dextrose is governed by size exclusion while that of EDCs are governed by both hydrophobic interactions in addition to size exclusion, this contrast in rejection behavior highlights the critical role of suppressing hydrophobic interactions by the selective pathways of MOFs for achieving enhanced EDCs rejection.

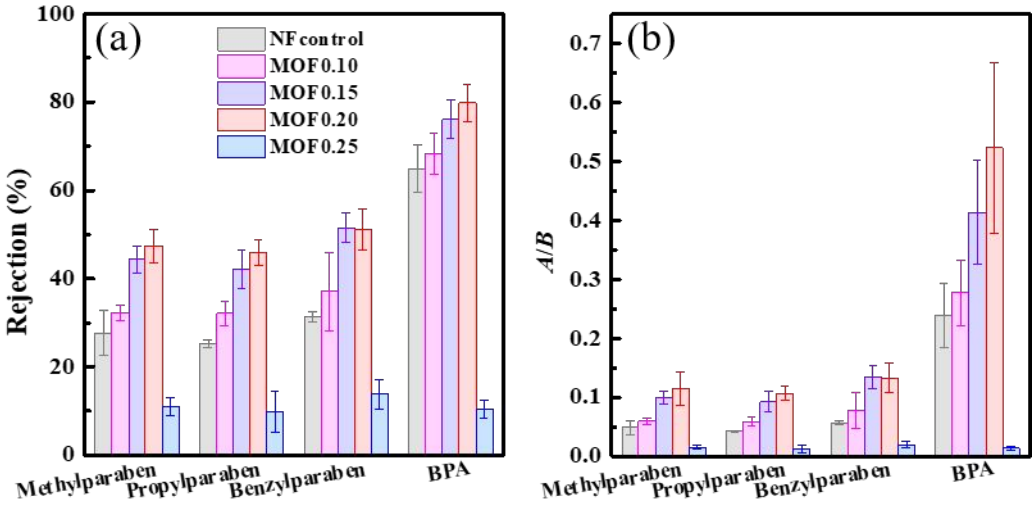


**Figure 4.** (a) The rejection and of EDCs and (b) water/EDCs selectivity (*A/B*) for NFcontrol and MOF-TFN membranes. The error bars represent the standard deviations of the results of three independent tests.

**Mechanistic Insights.** To better understand the underlying mechanisms, sorption of four EDCs by both NFcontrol and MOF-TFN membranes was conducted. We also determined the adsorption capacity of the EDCs at 200 μg/L by sole MIL-101(Cr) via Langmuir isotherm (SI, Section S12). Figure 5 indicates that all the modified membranes show a reduced rate of overall sorption against all the EDCs with the increase of MIL-101(Cr) incorporation. In general, MIL-101(Cr) MOFs had relatively low contribution to the adsorption of EDCs, which is consistent with its hydrophilic nature. The reduction in overall sorption for MOF-TFN membranes was largely attributed to the formation of more hydrophilic polyamide layers (Table 1). XPS analysis further suggests an increase of carboxylic groups on the MOF-loaded membrane surfaces as implied by the increased O/N ratios (Table S2), which is also consistent with their more hydrophilic membrane surfaces based on contact angle results. According to the solution-diffusion theory[42], the transport of a hydrophobic solute through a dense membrane is largely governed by its sorption onto the membrane, and its further diffusion in the membrane. Inverse correlation between the sorption of EDCs and its rejection by a NF membrane has been reported[10]. In the current study, the change in hydrophilicity of polyamide due to the incorporation of MIL-101(Cr) can reduce the sorption and mitigate the further transmission of EDCs across the membrane (Figure 6a, b).

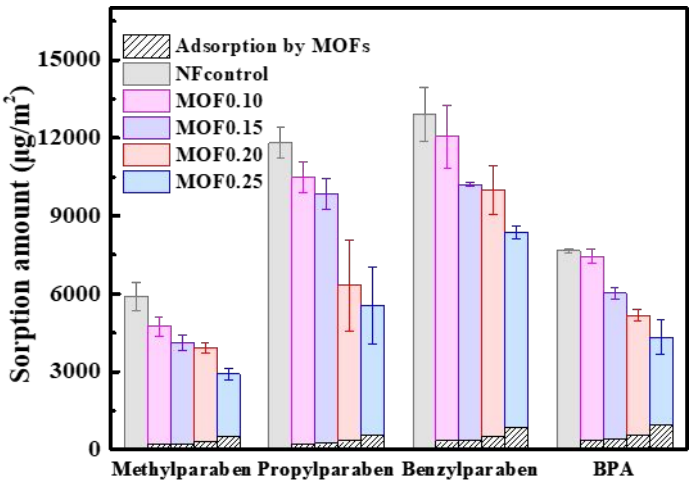


**Figure 5.** Contribution of MIL-101(Cr) and polyamide to sorption of EDCs on NFcontrol and MOF-TFN membranes. The error bars represent the standard deviations of the results of three independent tests.

Detailed analysis shows that MOF0.20 and NFcontrol had nearly identical solute permeability coefficients for the various EDCs (*B* values, Figure S9). Therefore, the enhanced rejection of EDCs by MOF0.20 can be considered as a direct consequence of the dilution effect: despite the similar solute flux of EDCs through the membrane, the significantly enhanced water transport through the selective nanochannels of MOFs resulted in reduced EDC concentrations in the permeate water (Figure 6). In a recent study, selective nanochannels were shown to form around hydrophilic AgNPs in a polyamide layer, which also increased the removal of hydrophobic compounds by suppressing hydrophobic interaction[39]. Nevertheless, compared to solid fillers such as AgNPs, MOFs of high porosity are capable of offering more abundant nanochannels, thus providing unique advantages over conventional solid nanofillers for selective removal of EDCs.

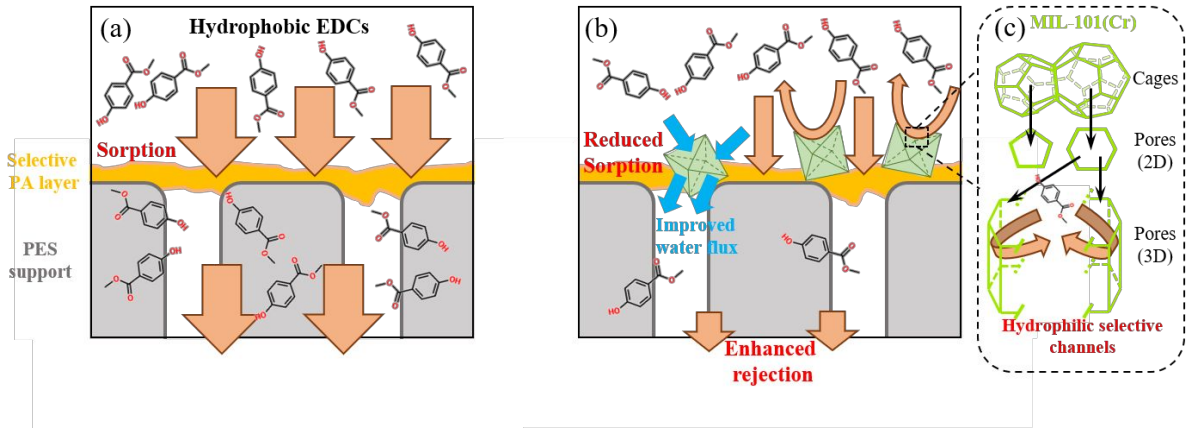


**Figure 6.** Schematic diagram of the mechanism of enhanced rejection of EDCs by MIL-101(Cr) in the polyamide layer. (a) EDC rejection by control membrane; (b) & (c) EDC rejection by the modified membrane.

**Implications.** Fabricating TFN membranes via incorporation of NPs is an effective way to break the trade-off between water and salt permeability[26–28]. However, the rejection of organic micropollutants (e.g., EDCs) is not well elaborated in the field of TFN membrane fabrication, despite their critical environmental significance and health concerns over common mineral salts such as NaCl in the context of wastewater reclamation[33]. In the current study, we enhanced the rejection of hydrophobic EDCs via incorporation of MOFs into a polyamide active layer. This enhancement was achieved without compromising the water permeability of the membrane, thereby overcoming the critical limitation of conventional enhancement methods by surface coating [10,22]. Indeed, the water permeability and water/EDCs selectivity of MOF0.20 membrane were both doubled compared to their respective values of the control, suggesting that the incorporation of MOFs into polyamide is an effective strategy to break the trade-off between water permeability and EDCs rejection.

In spite of the moderate enhancement in the rejection of EDCs, the mechanistic understanding gained from this study provides critical insights to guide the future development

and optimization of TFN membranes used for water reuse applications. For example, incorporating MOF materials with better selectivity and improving their dispersion at high loadings can likely lead to further improvement in EDC rejections. Together with their good membrane stability and the availability to treat EDCs-polluted real wastewater, as well as the stable long-term EDCs rejection performance (SI, Section S13-16), the novel engineered MIL-101(Cr) MOF-TFN membranes may have a great potential for toxic EDCs rejection and wastewater reclamation with low energy consumption.

The current study shows that MOFs can play a dominant role in the transport through TFN membranes. This offers exciting opportunities to tune the membrane separation performance by proper design/selection of the characteristics of MOFs. In this study, one important concern of the MIL-101(Cr)-loaded membranes is the reduced passage of divalent macrominerals such as $Ca^{2+}$, which is not favoured in potable water reuse applications[43]. Future studies may consider to further manipulate the charge properties of MOFs (e.g., by post-modification[44,45] such as the introduction of sulfonic acid groups[46]) to tune the rejection properties of ionic species. Moreover, besides the tunable pore charge, the adjustable pore size and flexible structure for MOFs [30–32] open a new paradigm to optimize the performance of MOF-TFN membranes in terms of rejecting micropollutants and a wide range of other contaminants.

## ASSOCIATED CONTENT

### Supporting information

The Supporting Information is available free of charge on the ACS Publications website at DOI:
Section S1. Calculations; S2. Building blocks of MIL-101(Cr); S3. Physicochemical properties and analytical method of selected EDCs; S4. Laboratory cross-flow filtration

setup; S5. MIL-101(Cr) Characterization; S6. SEM characterizations of membranes; S7. XPS results including elemental ratios of membranes; S8. Membrane pore size estimation for NFcontrol; S9. Dextrose (180 Da) rejections by membranes; S10. Static tests of gold nanoparticle deposition on MOF0.20; S11. Permeability of EDCs across membranes; S12. Sorption of EDCs by MIL-101(Cr); S13. Membrane stability; Section S14. Rejection of EDCs in real wastewater as background; Section S15. Long-term EDCs rejection performance; Section S16. Leaching and toxicity test of membranes and MOF.

## AUTHOR INFORMATION

*Corresponding Author*

*Tel.: +86-21-65975669, Fax: +86-21-65980400, E-mail address: zwwang@tongji.edu.cn

*Notes*

The authors declare no completing financial interest.

## ACKNOWLEDGMENTS

We thank the National Natural Science Foundation of China (Grant 51838009), the Peak Discipline Construction Program in Environment & Ecology of Shanghai and Shanghai Chengtou Wastewater Treatment Project (04002530949) for the financial support of the work.

## REFERENCES

(1) Shannon, M. A.; Bohn, P. W.; Elimelech, M.; Georgiadis, J. G.; Mariñas, B. J.; Mayes, A. M. Science and Technology for Water Purification in the Coming Decades. *Nature* **2008**, *452* (7185), 301–310. https://doi.org/10.1038/nature06599.

(2) Ma, J.; Dai, R.; Chen, M.; Khan, S. J.; Wang, Z. Applications of Membrane Bioreactors for Water Reclamation: Micropollutant Removal, Mechanisms and Perspectives. *Bioresource Technology* **2018**, *269*, 532–543. https://doi.org/10.1016/j.biortech.2018.08.121.

(3) Hering, J. G.; Ingold, K. M. Water Resources Management: What Should Be Integrated? *Science* **2012**, *336* (6086), 1234–1235. https://doi.org/10.1126/science.1218230.

(4) Boo, C.; Wang, Y.; Zucker, I.; Choo, Y.; Osuji, C. O.; Elimelech, M. High Performance Nanofiltration Membrane for Effective Removal of Perfluoroalkyl Substances at High Water Recovery. *Environmental Science & Technology* **2018**, *52* (13), 7279–7288. https://doi.org/10.1021/acs.est.8b01040.

(5) Tay, M. F.; Liu, C.; Cornelissen, E. R.; Wu, B.; Chong, T. H. The Feasibility of Nanofiltration Membrane Bioreactor (NF-MBR)+reverse Osmosis (RO) Process for Water Reclamation: Comparison with Ultrafiltration Membrane Bioreactor (UF-MBR)+RO Process. *Water Research* **2018**, *129*, 180–189. https://doi.org/10.1016/j.watres.2017.11.013.

(6) Soriano, Á.; Gorri, D.; Urtiaga, A. Efficient Treatment of Perfluorohexanoic Acid by Nanofiltration Followed by Electrochemical Degradation of the NF Concentrate. *Water Research* **2017**, *112*, 147–156. https://doi.org/10.1016/j.watres.2017.01.043.

(7) Peng, W.; Escobar, I. C. Rejection Efficiency of Water Quality Parameters by Reverse Osmosis and Nanofiltration Membranes. *Environmental Science & Technology* **2003**, *37* (19), 4435–4441. https://doi.org/10.1021/es034202h.

(8) Schäfer, A. I.; Nghiem, L. D.; Waite, T. D. Removal of the Natural Hormone Estrone from Aqueous Solutions Using Nanofiltration and Reverse Osmosis. *Environmental Science & Technology* **2003**, *37* (1), 182–188. https://doi.org/10.1021/es0102336.

(9) Verliefde, A. R. D.; Cornelissen, E. R.; Heijman, S. G. J.; Hoek, E. M. V.; Amy, G. L.; Bruggen, B. V. der; van Dijk, J. C. Influence of Solute−Membrane Affinity on Rejection of Uncharged Organic Solutes by Nanofiltration Membranes. *Environmental Science & Technology*. **2009**, *43* (7), 2400–2406. https://doi.org/10.1021/es803146r.

(10) Guo, H.; Deng, Y.; Tao, Z.; Yao, Z.; Wang, J.; Lin, C.; Zhang, T.; Zhu, B.; Tang, C. Y. Does Hydrophilic Polydopamine Coating Enhance Membrane Rejection of Hydrophobic Endocrine-Disrupting Compounds? *Environmental Science & Technology Letters* **2016**, *3* (9), 332–338. https://doi.org/10.1021/acs.estlett.6b00263.

(11) Kimura, K.; Toshima, S.; Amy, G.; Watanabe, Y. Rejection of Neutral Endocrine Disrupting Compounds (EDCs) and Pharmaceutical Active Compounds (PhACs) by RO Membranes. *Journal of Membrane Science* **2004**, *245* (1), 71–78. https://doi.org/10.1016/j.memsci.2004.07.018.

(12) Petrie, B.; Barden, R.; Kasprzyk-Hordern, B. A Review on Emerging Contaminants in Wastewaters and the Environment: Current Knowledge, Understudied Areas and Recommendations for Future Monitoring. *Water Research* **2015**, *72*, 3–27. https://doi.org/10.1016/j.watres.2014.08.053.

(13) Esperanza, M.; Suidan, M. T.; Nishimura, F.; Wang, Z.-M.; Sorial, G. A.; Zaffiro, A.; McCauley, P.; Brenner, R.; Sayles, G. Determination of Sex Hormones and Nonylphenol Ethoxylates in the Aqueous Matrixes of Two Pilot-Scale Municipal Wastewater Treatment Plants. *Environmental Science & Technology* **2004**, *38* (11), 3028–3035. https://doi.org/10.1021/es0350886.

(14) Wang, W.; Kannan, K. Fate of Parabens and Their Metabolites in Two Wastewater Treatment Plants in New York State, United States. *Environmental Science & Technology* **2016**, *50* (3), 1174–1181. https://doi.org/10.1021/acs.est.5b05516.

(15) Steinle-Darling, E.; Litwiller, E.; Reinhard, M. Effects of Sorption on the Rejection of Trace Organic Contaminants During Nanofiltration. *Environmental Science & Technology* **2010**, *44* (7), 2592–2598. https://doi.org/10.1021/es902846m.

(16) Yangali-Quintanilla, V.; Sadmani, A.; McConville, M.; Kennedy, M.; Amy, G. Rejection of Pharmaceutically Active Compounds and Endocrine Disrupting Compounds by Clean and Fouled Nanofiltration Membranes. *Water Research* **2009**, *43* (9), 2349–2362. https://doi.org/10.1016/j.watres.2009.02.027.

(17) Jin, X.; Hu, J.; Ong, S. L. Removal of Natural Hormone Estrone from Secondary Effluents Using Nanofiltration and Reverse Osmosis. *Water Research* **2010**, *44* (2), 638–648. https://doi.org/10.1016/j.watres.2009.09.057.

(18) Nghiem, L. D.; Schäfer, A. I.; Elimelech, M. Removal of Natural Hormones by Nanofiltration Membranes: Measurement, Modeling, and Mechanisms. *Environmental Science & Technology* **2004**, *38* (6), 1888–1896. https://doi.org/10.1021/es034952r.

(19) Hu, J.; Jin, X.; Ong, S. Rejection of Estrone by Nanofiltration: Influence of Solution

Chemistry. *Journal of Membrane Science* **2007**, *302* (1–2), 188–196. https://doi.org/10.1016/j.memsci.2007.06.043.

(20) Luo, Y.; Guo, W.; Ngo, H. H.; Nghiem, L. D.; Hai, F. I.; Zhang, J.; Liang, S.; Wang, X. C. A Review on the Occurrence of Micropollutants in the Aquatic Environment and Their Fate and Removal during Wastewater Treatment. *Science of The Total Environment* **2014**, *473–474*, 619–641. https://doi.org/10.1016/j.scitotenv.2013.12.065.

(21) Roepke, T. A.; Snyder, M. J.; Cherr, G. N. Estradiol and Endocrine Disrupting Compounds Adversely Affect Development of Sea Urchin Embryos at Environmentally Relevant Concentrations. *Aquatic Toxicology* **2005**, *71* (2), 155–173. https://doi.org/10.1016/j.aquatox.2004.11.003.

(22) Guo, H.; Yao, Z.; Yang, Z.; Ma, X.; Wang, J.; Tang, C. Y. A One-Step Rapid Assembly of Thin Film Coating Using Green Coordination Complexes for Enhanced Removal of Trace Organic Contaminants by Membranes. *Environmental Science & Technology* **2017**, *51* (21), 12638–12643. https://doi.org/10.1021/acs.est.7b03478.

(23) Guo, H.; Deng, Y.; Yao, Z.; Yang, Z.; Wang, J.; Lin, C.; Zhang, T.; Zhu, B.; Tang, C. Y. A Highly Selective Surface Coating for Enhanced Membrane Rejection of Endocrine Disrupting Compounds: Mechanistic Insights and Implications. *Water Research* **2017**, *121*, 197–203. https://doi.org/10.1016/j.watres.2017.05.037.

(24) Han, G.; Chung, T.-S.; Weber, M.; Maletzko, C. Low-Pressure Nanofiltration Hollow Fiber Membranes for Effective Fractionation of Dyes and Inorganic Salts in Textile Wastewater. *Environmental Science & Technology* **2018**, *52* (6), 3676–3684. https://doi.org/10.1021/acs.est.7b06518.

453 (25) Jeong, B.-H.; Hoek, E. M. V.; Yan, Y.; Subramani, A.; Huang, X.; Hurwitz, G.; Ghosh,
454 A. K.; Jawor, A. Interfacial Polymerization of Thin Film Nanocomposites: A New
455 Concept for Reverse Osmosis Membranes. *Journal of Membrane Science* **2007**, *294* (1–
456 2), 1–7. https://doi.org/10.1016/j.memsci.2007.02.025.
457 (26) Dai, R.; Zhang, X.; Liu, M.; Wu, Z.; Wang, Z. Porous Metal Organic Framework CuBDC
458 Nanosheet Incorporated Thin-Film Nanocomposite Membrane for High-Performance
459 Forward Osmosis. *Journal of Membrane Science* **2019**, *573*, 46–54.
460 https://doi.org/10.1016/j.memsci.2018.11.075.
461 (27) Wen, Y.; Chen, Y.; Wu, Z.; Liu, M.; Wang, Z. Thin-Film Nanocomposite Membranes
462 Incorporated with Water Stable Metal-Organic Framework CuBTTri for Mitigating
463 Biofouling. *Journal of Membrane Science* **2019**, *582*, 289–297.
464 https://doi.org/10.1016/j.memsci.2019.04.016.
465 (28) Zhu, J.; Qin, L.; Uliana, A.; Hou, J.; Wang, J.; Zhang, Y.; Li, X.; Yuan, S.; Li, J.; Tian,
466 M.; et al. Elevated Performance of Thin Film Nanocomposite Membranes Enabled by
467 Modified Hydrophilic MOFs for Nanofiltration. *ACS Applied Materials & Interfaces* **2017**,
468 *9* (2), 1975–1986. https://doi.org/10.1021/acsami.6b14412.
469 (29) Li, Y.; Wee, L. H.; Martens, J. A.; Vankelecom, I. F. J. Interfacial Synthesis of ZIF-8
470 Membranes with Improved Nanofiltration Performance. *Journal of Membrane Science*
471 **2017**, *523*, 561–566. https://doi.org/10.1016/j.memsci.2016.09.065.
472 (30) Li, J.-R.; Sculley, J.; Zhou, H.-C. Metal–Organic Frameworks for Separations. *Chem. Rev.*
473 **2012**, *112* (2), 869–932. https://doi.org/10.1021/cr200190s.
474 (31) Ma, D.; Han, G.; Peh, S. B.; Chen, S. B. Water-Stable Metal–Organic Framework UiO-

66 for Performance Enhancement of Forward Osmosis Membranes. *Ind. Eng. Chem. Res.* **2017**, *56* (44), 12773–12782. https://doi.org/10.1021/acs.iecr.7b03278.

(32) Sorribas, S.; Gorgojo, P.; Téllez, C.; Coronas, J.; Livingston, A. G. High Flux Thin Film Nanocomposite Membranes Based on Metal–Organic Frameworks for Organic Solvent Nanofiltration. *Journal of the American Chemical Society* **2013**, *135* (40), 15201–15208. https://doi.org/10.1021/ja407665w.

(33) Tang, C. Y.; Yang, Z.; Guo, H.; Wen, J. J.; Nghiem, L. D.; Cornelissen, E. Potable Water Reuse through Advanced Membrane Technology. *Environmental Science & Technology* **2018**, *52* (18), 10215–10223. https://doi.org/10.1021/acs.est.8b00562.

(34) Ferey, G. A Chromium Terephthalate-Based Solid with Unusually Large Pore Volumes and Surface Area. *Science* **2005**, *309* (5743), 2040–2042. https://doi.org/10.1126/science.1116275.

(35) Xu, Y.; Gao, X.; Wang, Q.; Wang, X.; Ji, Z.; Gao, C. Highly Stable MIL-101(Cr) Doped Water Permeable Thin Film Nanocomposite Membranes for Water Treatment. *RSC Advances* **2016**, *6* (86), 82669–82675. https://doi.org/10.1039/C6RA16896E.

(36) Marmur, A. Wetting on Hydrophobic Rough Surfaces: To Be Heterogeneous or Not To Be? *Langmuir* **2003**, *19* (20), 8343–8348. https://doi.org/10.1021/la0344682.

(37) Luo, J.; Wan, Y. Effects of PH and Salt on Nanofiltration—a Critical Review. *Journal of Membrane Science* **2013**, *438*, 18–28. https://doi.org/10.1016/j.memsci.2013.03.029.

(38) Szoke, S.; Patzay, G.; Weiser, L. Characteristics of Thin-Film Nanofiltration Membranes at Various PH-Values. *Desalination* **2003**, *151* (2), 123–129. https://doi.org/10.1016/S0011-9164(02)00990-6.

(39) Yang, Z.; Guo, H.; Yao, Z.; Mei, Y.; Tang, C. Y. Hydrophilic Silver Nanoparticles Induce Selective Nanochannels in Thin Film Nanocomposite Polyamide Membranes. *Environmental Science & Technology* **2019**, acs.est.9b00473. https://doi.org/10.1021/acs.est.9b00473.

(40) Pacheco, F. A.; Pinnau, I.; Reinhard, M.; Leckie, J. O. Characterization of Isolated Polyamide Thin Films of RO and NF Membranes Using Novel TEM Techniques. *Journal of Membrane Science* **2010**, *358* (1–2), 51–59. https://doi.org/10.1016/j.memsci.2010.04.032.

(41) Tan, Z.; Chen, S.; Peng, X.; Zhang, L.; Gao, C. Polyamide Membranes with Nanoscale Turing Structures for Water Purification. *Science* **2018**, *360* (6388), 518–521. https://doi.org/10.1126/science.aar6308.

(42) Wijmans, J. G.; Baker, R. W. The Solution-Diffusion Model: A Review. *Journal of Membrane Science* **1995**, *107* (1–2), 1–21. https://doi.org/10.1016/0376-7388(95)00102-I.

(43) Sedlak, D. L. The Unintended Consequences of the Reverse Osmosis Revolution. *Environ. Sci. Technol.* **2019**, *53* (8), 3999–4000. https://doi.org/10.1021/acs.est.9b01755.

(44) Kadhom, M.; Deng, B. Metal-Organic Frameworks (MOFs) in Water Filtration Membranes for Desalination and Other Applications. *Applied Materials Today* **2018**, *11*, 219–230. https://doi.org/10.1016/j.apmt.2018.02.008.

(45) Li, X.; Liu, Y.; Wang, J.; Gascon, J.; Li, J.; Van der Bruggen, B. Metal–Organic Frameworks Based Membranes for Liquid Separation. *Chemical Society Review* **2017**, *46* (23), 7124–7144. https://doi.org/10.1039/C7CS00575J.

519 (46) Zhang, Q.; Wahiduzzaman, M.; Wang, S.; Henfling, S.; Ayoub, N.; Gkaniatsou, E.; Nouar,
520 F.; Sicard, C.; Martineau, C.; Cui, Y.; et al. Multivariable Sieving and Hierarchical
521 Recognition for Organic Toxics in Nonhomogeneous Channel of MOFs. *Chem* **2019**, *5*
522 (5), 1337–1350. https://doi.org/10.1016/j.chempr.2019.03.024.

523